Inorganic Chemistry

pubs.acs.org/IC Article

Disclosing the Preferential Mercury Chelation by SeCys Containing Peptides over Their Cys Analogues

Mikel Bernabeu de Maria, Diego Tesauro, Filippo Prencipe, Michele Saviano, Luigi Messori, Christine Enjalbal, Ryszard Lobinski, and Luisa Ronga*

Cite This: *Inorg. Chem.* 2023, 62, 14980−14990 Read Online

ACCESS | Metrics & More | Article Recommendations | Supporting Information

ABSTRACT: Methylmercury, mercury (II), and mercury (I) chlorides were found to react with vasopressin, a nonapeptide hormone cyclized by two cysteine residues, and its mono- and diselenium analogues to form several mercury-peptide adducts. The replacement of Cys by SeCys in vasopressin increased the reactivity toward methylmercury, with the predominant formation of −Se/S−Hg−Se-bridged structures and the consequent demethylation of methylmercury. In competitive experiments, CH_3HgCl reacted preferentially with the diselenium analogue rather than with vasopressin. The diselenium peptide also showed the capability to displace the CH_3Hg moiety bound to S in vasopressin. These results open a promising perspective for the use of selenopeptides for methylmercury chelation and detoxification strategies.

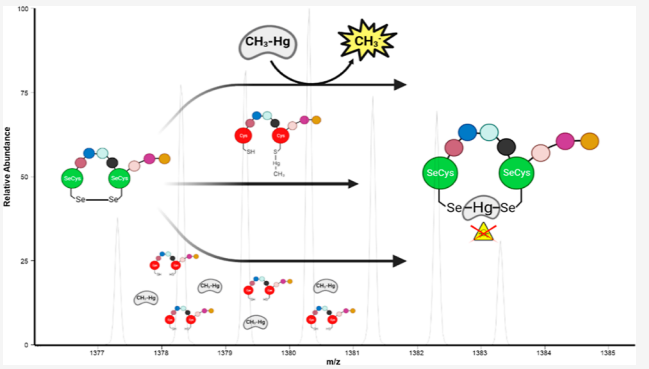

INTRODUCTION

Mercury (Hg), occurring in a number of inorganic [Hg(0), Hg(I), and Hg(II)] and organic (i.e., CH_3Hg^+) forms,[1,2] has been placed by the World Health Organization (WHO) on the list of top 10 most hazardous substances for humans, who are exposed mainly through dietary intake.[3,4] Mercury is classified as a soft element in the Pearson theory.[5] The affinity of Hg^{2+} and CH_3Hg^+ for the thiol group (soft base) of low- and high-molecular-weight biological ligands has been considered as the main reason for its high toxicity.[6]

Cysteine (Cys, C)-containing proteins and peptides are the primary targets for Hg^{2+} and CH_3Hg^+.[7] The coordination of Hg(II) to Cys is well described and results in the preferential formation of a stable linear Cys-Hg-Cys complex with the stability constant in a range of 10^{15} to 10^{42}.[8] The formation of other species displaying tri- and tetragonal geometries was also reported.[9] Moreover, the complexes formed between Hg(II) and linear and cyclic peptide scaffolds comprising typical metal-binding motifs, such as CxCxxC and CxCxC, found in metallothioneins and in the MerR metalloregulatory protein, show that the tri-thiolate coordination ($HgCys_3$) is the most frequent for these peptides at physiological pH.[10,11] A preference of Hg(II) for a di-thiolate binding (Cys-Hg-Cys) was evidenced in multi-cysteinyl peptides by mass spectrometry (MS)[12] and in several elements of Hg(II) transport proteins (MerP, MerT, and MerA), while tri- or tetra-coordinations were found in rubredoxin or in the MerR metalloregulatory protein dimer.[13−17]

More recently, it was found by X-ray photoelectron spectroscopy (XPS) that albumin, the main Hg(II)-binding protein in blood plasma, bound Hg(II) through a Cys-Hg-Cys coordination motif, while other Hg binding sites existed within the protein.[18]

The affinity of Hg(II) for thiol groups can provide some explanation for Hg toxicity pathways. For example, the close structural resemblance of CH_3Hg-L-cysteine complex with L-methionine[19] was reported to be partially responsible for its transport through the blood−brain and the placental barriers.[20,21] The covalent CH_3Hg^+-induced modification of thiol-containing biomolecules (the so-called "S-mercuration") was claimed responsible for the inactivation of several enzymes, such as the carnitine transporter[22,23] and the sorbitol dehydrogenase.[24] The Cys-mediated binding of CH_3Hg^+ and Hg^{2+} in proteins was also reported to induce apoptosis modulation by interfering with several metabolic pathways.[6]

The formation of complexes between Cys and Hg(I) has been less studied than that between Cys and Hg(II). Heyrovský et al. postulated the formation of a Cys-Hg-Hg-Cys complex and its subsequent transformation into Cys-Hg-Cys by addition of Cys, accompanied by the Hg oxidation from Hg(I) to Hg(II).[25]

Received: May 25, 2023
Published: August 31, 2023

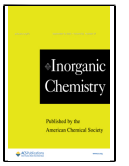

https://doi.org/10.1021/acs.inorgchem.3c01708
Inorg. Chem. 2023, 62, 14980−14990

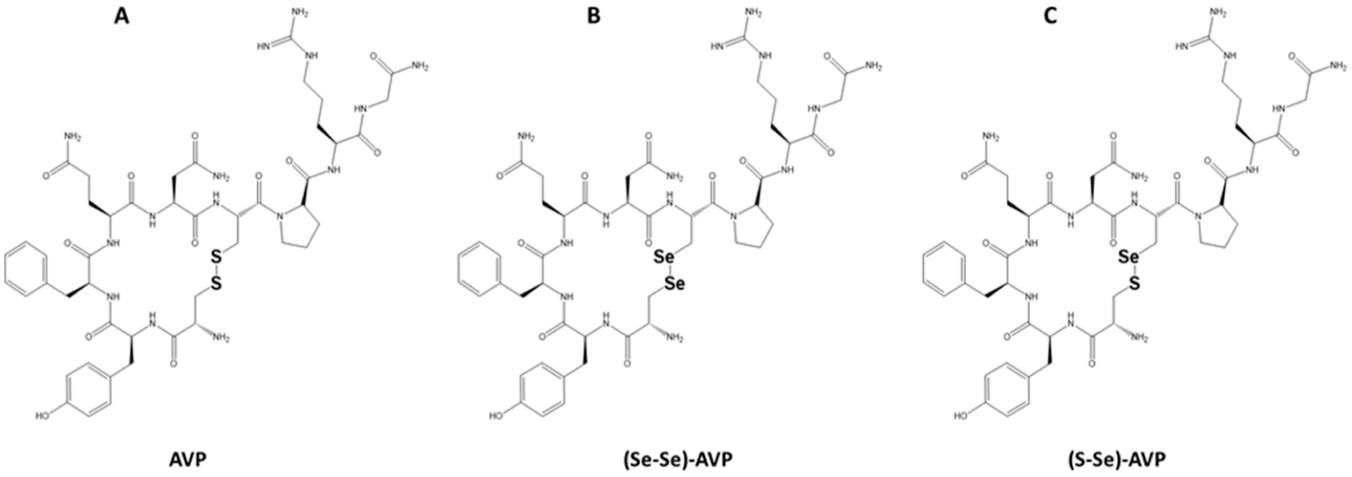

Figure 1. (**A**) Vasopressin (AVP), (**B**) diselenide (Se−Se)-AVP, and (**C**) selenylsulfide (S−Se)-AVP analogues.

Selenocysteine (SeCys, U), the 21st proteinogenic amino acid and the selenium (Se) analogue of cysteine, was also proposed as a Hg(II) target.[26] Although sulfur and selenium both belong to the chalcogen group (16), the selenol (−SeH) of SeCys is characterized by a softer character and higher nucleophilicity in comparison with the thiol (−SH) of Cys. Hg(II) affinity for −SeH is ca. 10^6 times larger than that for −SH, revealing selenium as the primary target of CH_3Hg^+.[27] Studies of the formation of complexes of Hg(II) compounds with SeCys have been scarce. Carty et al. reported on the characterization of the synthesized CH_3Hg-SeCys.[28,29] The synthetic CH_3Hg-seleno-glutathionate was characterized by NMR and X-ray spectroscopy and the comparison with its S-analogue did not show a significant change in the structure.[30] The formation of CH_3Hg−SeCys complexes was found to be thermodynamically more favorable than that of CH_3Hg−Cys compounds by quantum chemical calculations[31] but no experimental evidence was provided.

SeCys is genetically incorporated into selenoproteins (25 in humans), a class of proteins containing at least one SeCys,[32] but examples of the formal identification of the Hg(II)-SeCys moiety in peptide biomolecules have been rare and were limited to high-energy-resolution X-ray absorption near-edge structure (HR-XANES).[33] Tetraselenolate $Hg(SeCys)_4$ was identified in an animal tissue,[34] while Pickering et al. provided conclusive evidence for the binding of CH_3Hg^+ to Se in the selenoenzyme thioredoxin reductase 1 (TrxR1).[35] To the best of our knowledge, no selenopeptide model nor mimicry interacting with Hg compounds have been investigated. The comparative reactivity of Hg(II) toward Cys and SeCys has not been explored since the first study of Suguira et al. who used NMR to establish the following order of binding affinity to CH_3Hg^+: SeH > SH ≥ Se−Se > NH_2 > SS.[36]

The goal of this research was to investigate by liquid chromatography (LC) coupled to electrospray ultra-high-resolution mass spectrometry (ESI-MS) the competitive reactivity of a model disulfide peptide (vasopressin), and its mono- and diselenium analogues (Figure 1) toward methylmercury, mercury (II), and mercury (I) chlorides in the quest of potential mercury detoxification agents. Vasopressin (Figure 1A) is a nonapeptide hormone cyclized by two cysteine residues, best known for its antidiuretic and vasopressor actions. Its diselenide analogue [(Se−Se)-AVP, Figure 1B] was previously described,[37,38] and its selenylsulfide analogue [(S−Se)-AVP, Figure 1C] was synthesized for the purpose of this study. The elucidation of the Se−Hg binding sites was achieved by fragmentation of the reaction products in the gas phase (MS^n),[39] as proposed elsewhere for the study of the reactivity of AVP and (Se−Se)-AVP peptides with medicinally relevant gold compounds.[40]

EXPERIMENTAL SECTION

Materials. Dithiothreitol (DTT), ammonium acetate, acetic acid, ammoniac, acetonitrile (ACN), methyl mercury chloride (CH_3HgCl), and mercury chloride ($HgCl_2$) were purchased from Sigma-Aldrich. Formic acid (FA) was purchased from Thermo Fisher Scientific. Mercury (I) chloride (Hg_2Cl_2) was provided by Pr. Luigi Messori.

AVP [high-performance liquid chromatography (HPLC) purity 98%] was purchased from Eurogenetec (Research, Dioagnostics, & Therapeutic Solutions, located in Seraing, Belgium). (Se−Se)-AVP (HPLC purity 97%) was synthesized as previously described[37,38] and (S−Se)-AVP (HPLC purity 95%) was synthesized as described here.

Fmoc-protected amino acid derivatives, coupling reagents (*O*-benzotriazole-*N*,*N*,*N*′,*N*′-tetramethyluroniumhexafluorophosphate (HBTU, purity ≥99%), hydroxybenzotriazole (HOBt, purity ≥97.5%), and resin (Rink amide *p*-methylbenzhydrylamine MBHA 0.78 mmol/g) were purchased from Calbiochem−Novabiochem (Laufelfingen, Switzerland). Seleno-L-cystine (purity 95%), m-Cresol (purity 98%), thioanisole (purity ≥99%), trifluoroacetic acid (purity ≥99%), trimethylsilyl trifluoromethanesulfonate (purity ≥98%), Kaiser test kit (ninhydrin test to detect free amino acids), TLC Silica Gel 60 (0.075−0.2 mM particle size, mesh 70−200), aluminum sheets, and all other solvents and reagents were purchased from Sigma-Aldrich, Steinheim, Germany. All the chemicals were used as received without further purification.

Warning: methylmercury and other Hg (II) and Hg(I) forms are highly toxic and must be handled with appropriate personal protection. This requires the use of highly resistant laminate gloves, use of a fume hood, and approved breathing apparatus.

Methods. *(S−Se)-AVP Peptide Synthesis.* In order to perform the solid phase synthesis of the (S−Se)-AVP peptide, an orthogonally protected SeCys building block is prepared, as reported in Schemes 1 and 2 and then incorporated on the growing peptide chain.

Synthesis of Se-4-Methoxybenzylseleno-L-cysteine.[41] Seleno-L-cystine (334 mg, 1 mmol) was suspended in 1 mL of 0.500 M NaOH. The mixture was cooled in an ice bath, and then a solution of $NaBH_4$ (306 mg, 8.1 mmol) dissolved in water (2 mL) was added dropwise. The reaction is vigorous and develops H_2 (as the reaction proceeds the color changes from yellow to white and gradually a colorless solution was obtained). At the end of the gas evolution, glacial acetic acid was added up to pH 6 (also in this case, the reaction is vigorous). *p*-Methoxybenzyl chloride (PMB) (202 μL, 2 mmol) was

https://doi.org/10.1021/acs.inorgchem.3c01708
Inorg. Chem. 2023, 62, 14980−14990

Scheme 1. Synthesis of Se-4-Methoxybenzylseleno-L-cysteine (SeCys(MBzl)) from Seleno-L-cystine

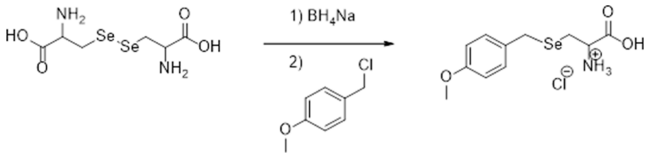

Scheme 2. Synthesis of N-9-Fluorenylmethoxycarbonyl-Se-4-methoxybenzylselenocystein (Fmoc-SeCys(MBzl)) from SeCys(MBzl)

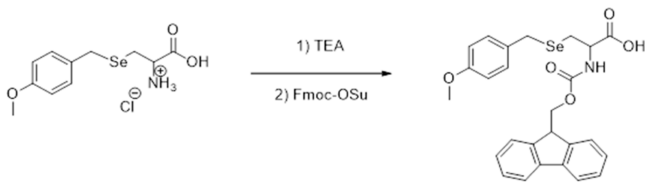

added dropwise and the mixture left under stirring at room temperature. The reaction is fast and takes about 30 min to complete. It was acidified with HCl 37% to favor the precipitation of the product (cool in an ice bath). The precipitate was filtered and recrystallized from hot water to give a white solid. The pure compound was analyzed by ^{1}H NMR in $(CD_3)_2SO$ (Figure S11) and ESI-MS (Figure S12).

^{1}H NMR (400 MHz, $(CD_3)_2SO$ DMSO-d_6): δ 8.54 (br s, 3H), 7.26 (d, J = 8.6 Hz, 2H), 6.87 (d, J = 8.7 Hz, 2H), 3.88 (s, 3H), 3.70 (s, 2H), 2.94 (m, 2H). Formula: $C_{11}H_{16}NO_3Se$, calculated mass 289.2. MS (ESI^+) m/z: 290.2.

Synthesis of N-9-Fluorenylmethoxycarbonyl-Se-4-methoxybenzylselenocystein. To a suspension of SeCys(MBzl) (150 mg, 0.517 mmol) in water (2 mL) was added 1 equiv of triethylamine (TEA) at room temperature. Subsequently, Fmoc-OSu, solubilized in CH_3CN (2 mL), was added dropwise to the reaction mixture.

Another equivalent of TEA and 6 mL supplementary of CH_3CN were added to obtain a clear solution (about 8 mL). The solution was left under stirring at room temperature for 1.5 h (monitored during this reaction time by silica TLC, DCM/CH_3OH 9: 1, Rf. Product = 0.5).

It was acidified with 1N HCl (1.5 mL) and extracted with ethyl acetate (3 × 20 mL). The organic extracts were combined, washed with brine (high-concentration solution of NaCl), anhydrified with Na_2SO_4, and dried under vacuum. The obtained oily residue was purified by chromatography on a Silica Gel 60 using a packed 40 cm × 5 cm column, 0.075−0.2 mm (70−200 mesh). The elution was performed by 100% $CHCl_3$ to remove impurities and subsequently by a mixture of $CHCl_3$/CH_3OH 9.5:0.5 v/v. The obtained pure white solid was characterized by ^{1}H and ^{13}C NMR in $(CD_3)_2SO$ (Figures S13 and S14, respectively).

^{1}H NMR (400 MHz, $(CD_3)_2SO$): δ 7.90 (d, J = 7.5 Hz, 2H), 7.74 (d, J = 7.8 Hz, 2H), 7.42 (t, J = 7.4 Hz, 2H), 7.32 (ddd, J = 9.1, 5.2, 1.8 Hz, 2H), 7.21 (d, J = 8.5 Hz, 2H), 6.84 (d, J = 8.5 Hz, 2H), 4.34−4.15 (m, 4H), 3.80 (s, 2H), 3.72 (s, 3H), 2.86−2.70 (m, 2H). **^{13}C NMR** (101 MHz, $(CD_3)_2SO$): δ 172.86, 158.40, 156.40, 144.26, 141.18, 131.64, 130.36, 128.12, 127.55, 125.77, 120.59, 114.24, 66.19, 55.48, 55.01, 47.08, 26.76, 24.84.

^{1}H NMR and ^{13}C NMR spectra were acquired with a Brucker 400 MHz.

Solid Phase Peptide Synthesis of (S−Se)-AVP. The peptide was synthesized manually via the Fmoc protocol on a 0.1 mmol scale using a Rink amide resin (0.78 mmol/g). 128 mg of resin were swelled for 30 min in dichloromethane and the Fmoc cleaved from the resin by adding 5 mL of 20% (v/v) piperidine in dimethyl formamide (DMF). The resin was left 30 min under stirring in the 20% piperidine solution. The Fmoc deprotection protocol was repeated twice. Then, the commercial Fmoc-protected residues and the synthetized Fmoc-SeCys(MBzl) were coupled stepwise to the resin by using the following protocol. A fivefold excess of Fmoc amino acid, HBTU, and HOBt were (i) solubilized in 10 mL of 0.2 M *N*,*N*-diisopropylethylamine (DIEA)/DMF solution, (ii) left under stirring for 5 min (amino acid pre-activation), (iii) added to the resin, and (iv) left 2 h under reaction. The protocol of amino acid coupling was repeated twice for each residue before proceeding with the Fmoc deprotection achieved by adding to the resin 5 mL of 20% (v/v) piperidine in DMF (5 min under stirring, twice). After each amino acid coupling and Fmoc deprotection protocols, the resin was washed 3 times with 10 mL of DMF. A Kaiser test kit (ninhydrin test kit) was used for the detection of free amino functional groups and the determination of the completion of amino acid coupling reactions.[42] Cleavage of peptide from the resins was carried out adapting the method reported by Hondal et al.:[43] 8 h at room temperature under stirring with a cleavage cocktail (1 mL of mixture for g of resin) made by *m*-cresol/thioanisole/trifluoroacetic acid/trimethylsilyl trifluoromethanesulfonate (50:120:690:194). Then, the mixture was filtered from the resin and evaporated to one-tenth of its original volume under a stream of nitrogen followed by precipitation of peptides into cold anhydrous diethyl ether. A crude peptide was lyophilized and then purified by HPLC as outlined below. The pure peptide was lyophilized recovering 50 mg (42.4% yield) and analyzed by ESI-MS (Figures S15 and S16). We found the expected value of $[M + H]^+$ = 1132.3887 Da and $[M + 2H]^{2+}$ = 566.6982 Da.

Preparative HPLC was carried out on a LC8 Shimadzu HPLC system (Shimadzu Corporation, Kyoto, Japan) equipped with a UV lambda-Max model 481 detector using a Phenomenex (Torrance, CA) C18 (300 Å, 250 × 21.20 mm, 5μ) column eluted with H_2O/0.1% TFA (A) and ACN/0.1% TFA (B) from 20−80% over 15 min at a flow rate of 2.0 mL·min^{-1}.

Purity of products was assessed using analytical HPLC (Agilent), column: C18-Phenomenex eluted with an H_2O/0.1% TFA (A), and ACN/0.1% TFA (B) from 5% to 80% over 20 min at 1 mL/min flow rate.

LC−MS STUDY

Sample Preparation. Stock solutions of AVP, (Se−Se)-AVP, (S−Se)-AVP 0.9 mM, and DTT 0.2 M were prepared by dissolving the samples in ultrapure water. Ammonium acetate buffer solution (2 mM, pH 7.0) was prepared by weighing ammonium acetate and dissolving it in ultrapure water, pH adjustment was carried out with acetic acid and ammonia commercial solutions (35% NH_3). For the incubation with mercury (II) compounds, 10 mM stock solutions of CH_3HgCl and $HgCl_2$ were prepared by dissolving salts in ultrapure water (0.1% HCl). For the pre-reduction of peptides, aliquots of their stock solution were diluted with 2 mM ammonium acetate solution (pH 7.0) to 0.1 mM final peptide concentration. Then, aliquots of DTT stock solution were added to achieve a peptide to reducing agent ratio of 1:10 (final concentration of 1 mM of reducing agent), and the mixtures were incubated for 30 min at 37 °C in a water bath under stirring. Thereafter, aliquots of CH_3HgCl and $HgCl_2$ stock solution were added to achieve the peptide to Hg ratios of 1:1, 1:2, and 1:3 (0.1, 0.2, and 0.3 mM, Hg concentration, respectively). Those mixtures were explored over different incubation times (from 30 min up to 18 h) at 37 °C.

After the incubation, all mercury (II)-incubated solutions were sampled and diluted to a final peptide concentration of 6 μM, using 2 mM ammonium acetate pH 7, 5% (v/v) of ACN, and 0.1% (v/v) FA used for LC−MS analysis.

For the incubation with Hg_2Cl_2, a saturated stock solution was prepared by dissolving 0.1 mg of calomel in 50 mL of ultrapure water (4.2 μM Hg_2Cl_2 concentration). Then, 1 mL of this solution was mixed with 14 μL of reduced peptide at 0.1 mM in 2 mM ammonium acetate solution pH 7 (approximately, 1:3, peptide to Hg(I) ratio), incubated for 18 h, and then analyzed by LC−MS.

https://doi.org/10.1021/acs.inorgchem.3c01708
Inorg. Chem. 2023, 62, 14980−14990

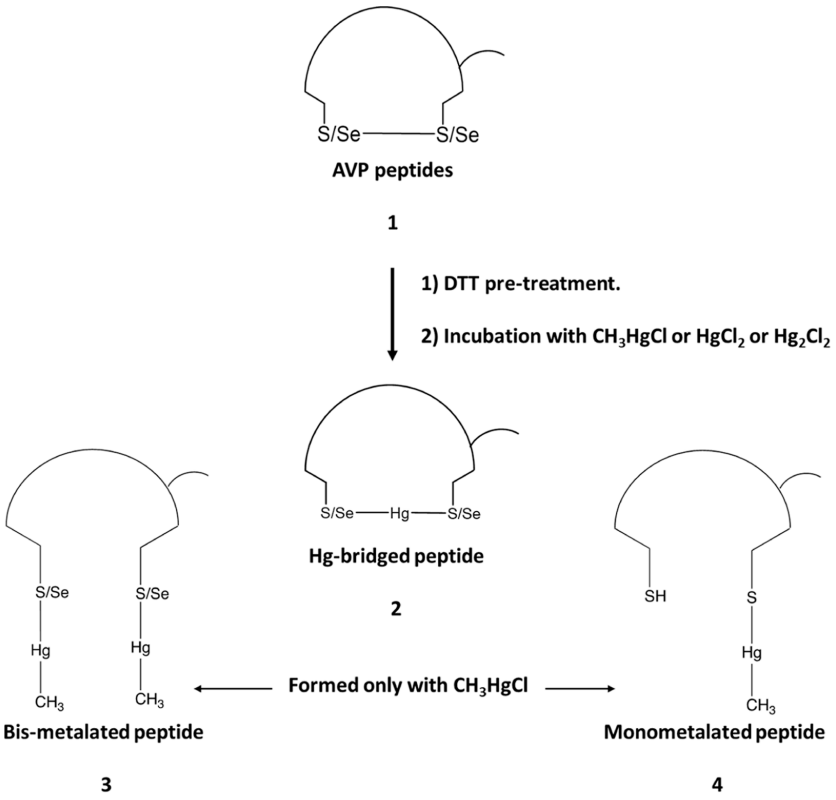

Figure 2. Scheme of the experiments: AVP peptides incubated with CH_3HgCl, $HgCl_2$, or Hg_2Cl_2 promoting, in the presence of DTT, the formation of Hg-bridged peptide adducts, and, with CH_3HgCl, also the mono- and bis-metalated complexes.

For the competitive study, the same starting solutions of peptides and CH_3HgCl were used and the same peptide concentration was employed for both incubation and LC−MS analysis.

LC-ESI MS

Separation and identification of our samples was performed by LC-ESI MS. Liquid chromatography separations were performed using a Dionex ultimate 3000 series UHPLC (Thermo Fisher Scientific) coupled to an Orbitrap Q-Exactive Plus mass spectrometer (Thermo Fisher Scientific). The used column was an AcclaimTM 120 (C18, 5 μm, 120 Å, 4.6 mm × 100 mm) (Thermo Fisher Scientific). The mobile phases were A, H_2O, and B, ACN, both with 0.1% FA. The flow rate used in all LC−MS experiments was 1 mL·min^{-1}, and sample elution was performed by using the gradient from 5 to 95% of B over 6.5 min. An injection volume of 10 μL was used.

Ionization was performed using an electrospray ion source operating in the positive ion mode with a capillary voltage of 3.80 kV and capillary temperature of 400 °C. Sheath gas, auxiliary gas, and sweep gas flow rate were set at 75, 20, and 1 (arbitrary units), respectively. The auxiliary gas temperature was set at 500 °C.

For each studied mass, a set of MS/MS spectra were acquired using an isolation width of 1.0 and 7.0 m/z, and a screening of collision energies (from 10 to 40 values of higher energy collisional dissociation (HCD)) was carried out. All MS data were analyzed using a Thermo Fisher Scientific Xcalibur the Qual Browser and FreeStyle software.

LC-ICP MS

Using the same chromatographic delivery system as previously described in the LC-ESI MS methodology, a Dionex ultimate 3000 series UHPLC pump was coupled to a NexION 5000 inductively coupled mass spectroscopy (ICP MS) (Perkin Elmer) fitted with platinum cones. The exit of the column was connected to the nebulizer of a multiquadrupole ICP MS instrument, which allowed us to work in the MS/MS mode. Employed carrier gas and option gas flow (O_2, used for avoiding carbon deposition from the organic mobile phase) were 0.78 and 0.08 mL·min^{-1}, respectively. Hg was analyzed in "on-mass mode", i.e., filtering the m/z = 202 in Q1 and Q3 and RPq 0.25; while Se was analyzed in the "mass-shift" mode, filtering the m/z = 80 in Q1 and m/z = 96 in Q3 after reaction with O2, and RPq 0.8. The total acquisition time was 600 s.

Data Treatment. The ESI MS sensitivity, which is different for the different metal complexes, was normalized using the ICP MS sensitivity (for selenium), which is independent of the peptide. This resulted in the following correction factors: 0.76 for **1** (unreacted peptide), 5.25 for **2** (Hg-bridged peptide), 0.88 for **3** (bis-metalated adduct), and 2.30 for **4** (monometalated peptide). Note that this approach could not be used for AVP that did not contain Se because the ICP quantification of sulfur was hampered by the presence of DTT in the reaction medium. In these cases, an assumption was made that the ionization of the S peptides was the same as that of their Se analogues. The above correction factors are applied to the relative abundances in Figures S20−22, S26−28, and S32 in order to make the graphics of Figures 5−7.

https://doi.org/10.1021/acs.inorgchem.3c01708
Inorg. Chem. 2023, 62, 14980−14990

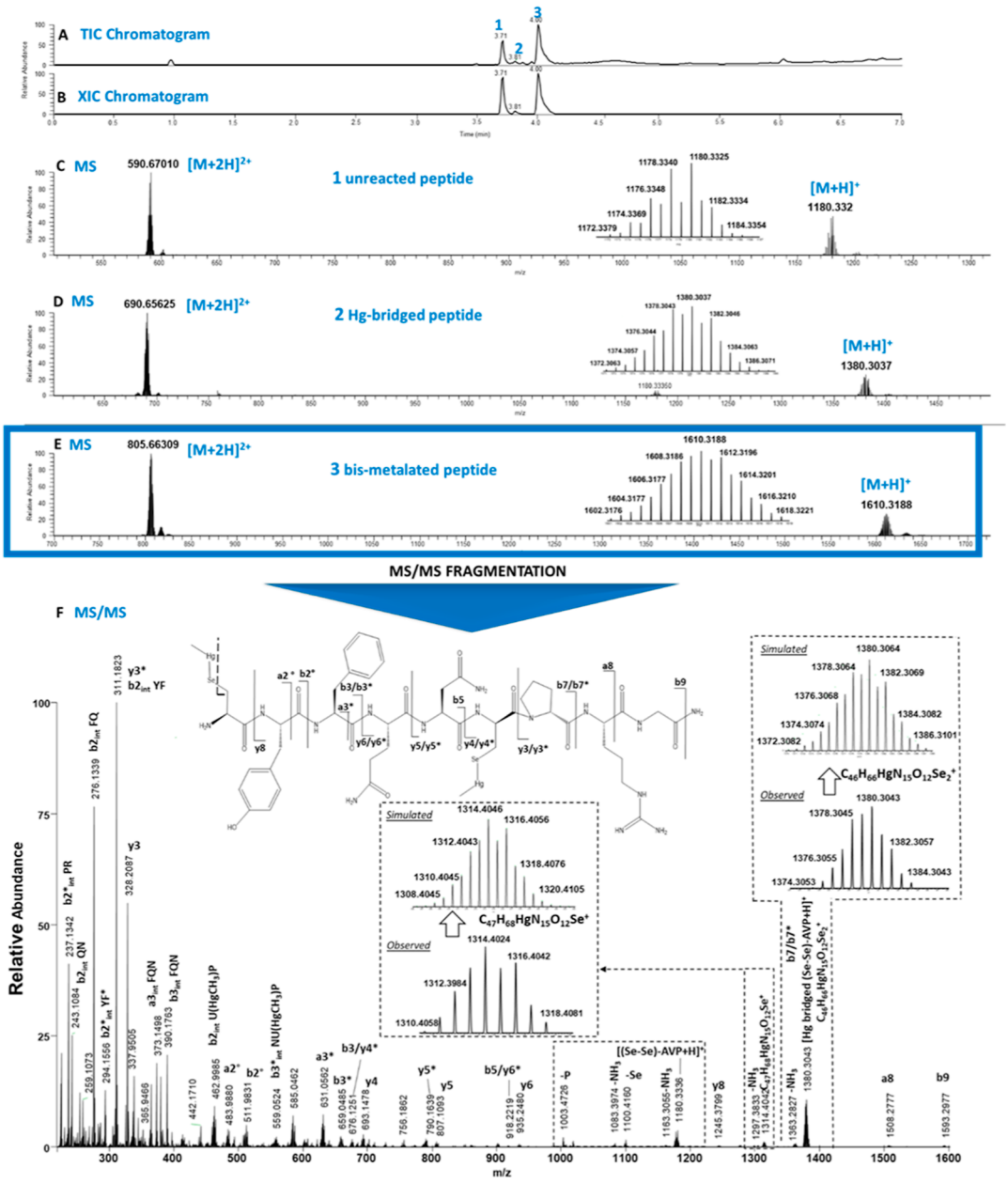

Figure 3. LC−MS of (Se−Se)-AVP incubated with 1 equiv of CH_3HgCl at 37 °C in the presence of DTT after 30 min. (**A**) TIC. (**B**) XIC of ions m/z 590.67 ($z = 2$, **1** unreacted peptide and $t_R = 3.69$), 690.65 ($z = 2$, **2** Hg-bridged peptide, $t_R = 3.79$), and 805.66 ($z = 2$, **3** bis-metalated peptide, $t_R = 3.99$). (**C**−**E**) MS spectra of **1** unreacted peptide, $t_R = 3.69$, **2** Hg-bridged peptide, $t_R = 3.79$, and **3** bis-metalated peptide, $t_R = 3.99$, respectively. (**F**) MS/MS of **3** bis-metalated peptide at m/z 1610.3190 ($z = 1$), principal fragments at higher energy collisional dissociation (HCD) = 30.

RESULTS AND DISCUSSION

Principle of the LC−MS/MS Approach. As depicted in Figure 2, the three model AVP peptides were pretreated (30 min at 37 °C) with the reducing agent dithiothreitol (DTT) and then reacted at physiological conditions (pH 7 and 37 °C) with $HgCl_2$, CH_3HgCl, or Hg_2Cl_2 (calomel), at different peptide/Hg molar ratios (from 1 to 3 equiv) and incubation times (from 30 min to 18 h) leading to several metal-peptide adducts (Tables 1 and S1).

The reaction products were monitored and identified by LC−MS/MS (Figures S17−19, S23−25 and S29−31); their identification was also complemented by comparison of experimental and theoretical isotopic patterns (Figures S1−8). The typical set of results [an example is shown in Figure 3 for (Se−Se)-AVP incubated with CH_3HgCl (1 equiv, 30 min)] consisted of a total ion current chromatogram (TIC), mass spectra taken at the peak apexes (MS), the relative intensity of each species at their characteristic m/z values [extracted ion chromatogram, (XIC)], and their MS/MS spectra used to elucidate the metal binding sites. In brief, in Figure 3, the TIC peaks 1, 2, and 3 (Figure 3**A**) were identified in mass spectra (Figure 3**C**−**E**) as the unreacted, the Hg-bridged, and the bis-metalated (Se−Se)-AVP peptides, respectively. The MS/MS of bis-metalated peptide (Figure 3**F**) revealed the direct involvement of Se in the binding with mercury. Moreover, on the basis of the intensity of the XIC of each species ($z = 2$, $[M + 2H]^{2+}$) (Figure 3**B**), we were able to assess the relative abundance of each of these peptides in the reaction medium as follows: 51 ± 1.6% of **3** (bis-metalated adduct), 45 ± 1.7% of **1** (unreacted

https://doi.org/10.1021/acs.inorgchem.3c01708
Inorg. Chem. 2023, 62, 14980−14990

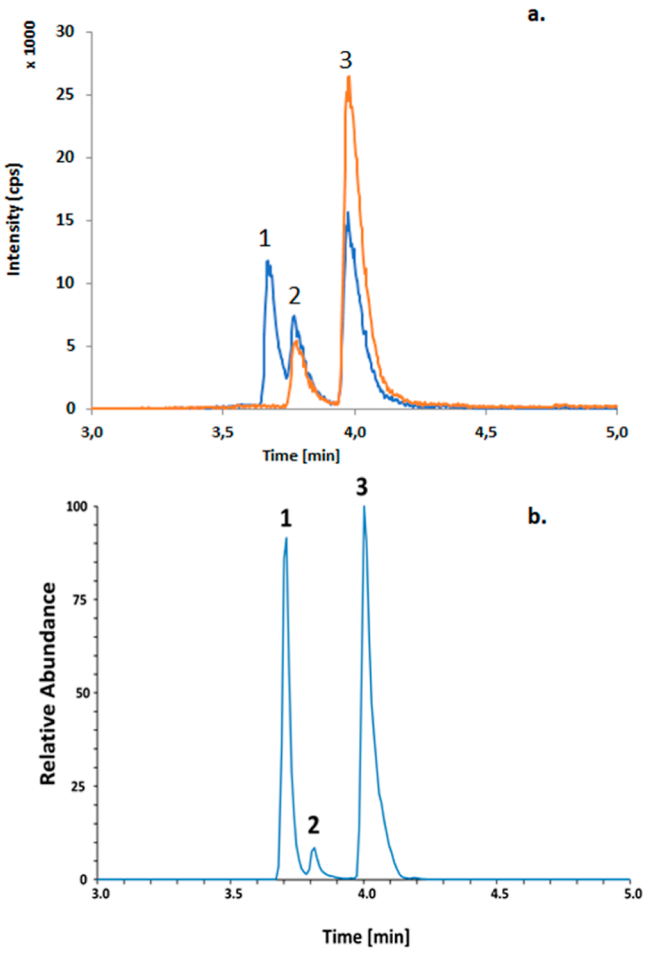

Figure 4. LC-ESI MS and LC-ICP MS/MS of (Se−Se)-AVP incubated with 1 equiv of CH_3HgCl at 37 °C in the presence of DTT after 30 min. (**a**) ICP−MS/MS detection: Se (blue line ^{96}Se ICP intensity) and Hg (orange line ^{202}Hg ICP intensity). (**b**) ESI-MS detection: XIC of ions m/z 590.67 (**1** unreacted peptide, t_R = 3.71 min), 690.65 (**2** Hg-bridged peptide, t_R = 3.81 min), and 805.66 (**3** bis-metalated peptide, t_R = 4.00 min).

peptide), and 4.0 ± 0.2% of **2** (Hg-bridged peptide), these standard deviation values were found to be lower than expected.

As the ESI-MS sensitivity can be different for the different metal complexes, it may need to be normalized for the purpose of comparison. This normalization can be done by integrating an ICP MS detection in HPLC into the approach, as outlined in Figure 3. In contrast with ESI-MS detection, ICP−MS is an element specific detector offering a response independent of the molecular structure of a peptide.[40] Figure 4 shows a set of chromatograms with the parallel ICP−MS and ESI-MS detection obtained for the analysis of the same reaction medium on which the developed normalization approach was based. The approach allowed one to calculate the correction factors, which are given in the aforementioned Data Treatment section.

Note that metalation took place only when the peptides were pre-treated with DTT. This classical reduction protocol, which was tested to promote the reactivity of free selenols and thiols with mercury compounds, was able to reduce the disulfide bond of AVP but not the diselenide bond[44] nor the S−Se bond. Our results, therefore, demonstrate the synergistic effect of DTT in promoting the reaction of Se with different Hg compounds when still present in the Se−Se form rather than in the selenol form. A competitive reactivity of DTT with the tested mercury compounds was found only in the case of AVP peptide incubations with CH_3HgCl: only traces of DTT-Hg adduct formation were detected in these reaction media (Figures S17−19 and S9−10).

AVP Peptide Reactivity with CH_3HgCl. The reaction of the three AVP peptides with CH_3HgCl produced the mono-, bis-metalated, and the Hg-bridged adducts (cf. Figure 2). These adducts were characterized by MS/MS revealing the direct involvement of Cys and SeCys in the binding with mercury (Figures S37−45).

Figure 5 shows for each peptide the relative abundance of unreacted and metalated peptides as a function of the number of CH_3HgCl equivalents at the different reaction times. These percentages were measured on the basis of the intensity of the extracted ion chromatogram for each reaction product (m/z with z = 2) (Figures S20−22), by applying the ICP-related correction factors as previously described.

The results of AVP metalation were similar at the different incubation times; the peptide was mainly transformed into **4**: the monometalated peptide adduct. By increasing the excess of CH_3HgCl, the conversion of the starting peptide into the monometalated adduct increased, but unreacted peptide **1** still remained after 18 h incubation with 3 equiv of CH_3HgCl.

(Se−Se)-AVP was largely converted into Hg adducts already at 30 min of incubation in the presence of 1 equiv of CH_3HgCl: the bis-metalated adduct **3** was largely formed together with the Hg-bridged form **2**. At any reaction time, when the excess of CH_3HgCl increased, the starting peptide reacted almost completely, and the quantity of the bis-metalated adduct decreased by favoring the formation of Hg-bridged peptide **2**.

The (S−Se)-AVP peptide showed an almost quantitative conversion into Hg adducts after 30 min of incubation with 1 equiv of CH_3HgCl by forming similar quantities of the Hg-bridged peptide **2**, the mono- **4**, and bis-metalated **3** adducts. Like in the case of (Se−Se)-AVP, at longer incubation time, the Hg-bridged peptide **2** represented the most predominant form of Hg-peptide adduct.

AVP Peptide Reactivity with $HgCl_2$. The reaction of the three AVP peptides with $HgCl_2$ produced exclusively the Hg-bridged adduct **2** (cf. Figure 2).

Figure 6 shows for each peptide the relative abundance of unreacted peptide and Hg-bridged adduct as a function of the number of $HgCl_2$ equiv at the different reaction times. These percentages were measured on the basis of the intensity of the extracted ion chromatogram of each reaction product (m/z with z = 2) (Figures S26−28), by applying the ICP-related corrections factors as previously described.

AVP showed similar reactivity profiles regardless of the excess of $HgCl_2$ or of the reaction time: the metalation was almost quantitative.

(Se−Se)-AVP needed a longer incubation time to be almost totally metalated, while (S−Se)-AVP, as well as AVP, showed high conversion to the Hg-bridged adduct at any excess of $HgCl_2$ or reaction time.

AVP Peptide Reactivity with Hg_2Cl_2. In the case of Hg_2Cl_2, experiments were hampered by the low solubility of calomel in aqueous solution[45] making the precise control of Hg excess at low concentrations impossible. Therefore, incubations were performed exclusively in the presence of an excess of calomel (approximately, 3 equiv, at 4.2 μM concentration) during 18 h.

https://doi.org/10.1021/acs.inorgchem.3c01708
Inorg. Chem. 2023, 62, 14980−14990

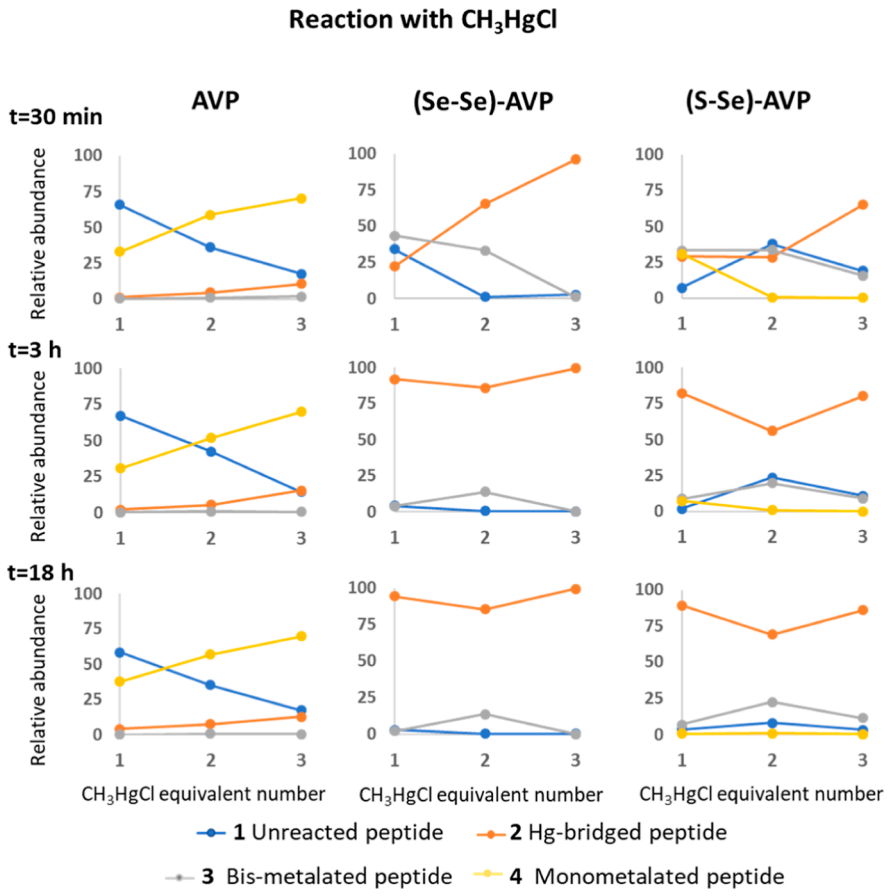

Figure 5. AVP peptides incubated at 37 °C in the presence of DTT with CH_3HgCl (1−3 equiv) at 30 min, 3 and 18 h. Percentage of unreacted and metalated peptides are reported as a function of CH_3HgCl excess at the different reaction times.

Table 1. AVP Peptides and Their Hg Adducts Identified by Mass Spectrometry after Incubation of the Peptides with $HgCl_2$, CH_3HgCl, or Hg_2Cl_2

Peptide	Formula	Theoretical mass of the most abundant isotope ($Se^{79.9160}$ and $Hg^{201.9701}$) Da	Experimental mass of the most abundant isotope ($Se^{79.9160}$ and $Hg^{201.9701}$) Da	$\Delta M_{theor-exp}$ Da
AVP	$C_{46}H_{65}N_{15}O_{12}S_2$	1083.4373	1083.4368	0.0005
Reduced AVP	$C_{46}H_{67}N_{15}O_{12}S_2$	1085.4530	1085.4525	0.0005
Hg-bridged AVP[a]	$C_{46}H_{65}HgN_{15}O_{12}S_2$	1285.4083	1285.4090	−0.0007
Bis-metalated AVP[b]	$C_{48}H_{71}Hg_2N_{15}O_{12}S_2$	1515.4243	1515.4236	0.0007
Monometalated AVP[b]	$C_{47}H_{69}HgN_{15}O_{12}S_2$	1301.4397	1301.4525	−0.0128
(Se−Se)-AVP	$C_{46}H_{65}N_{15}O_{12}Se_2$	1179.3274	1179.3266	−0.0009
Hg-bridged (Se−Se)-AVP[a]	$C_{46}H_{65}HgN_{15}O_{12}Se_2$	1379.2980	1379.2978	0.0002
Bis-metalated (Se−Se)-AVP[b]	$C_{48}H_{71}Hg_2N_{15}O_{12}Se_2$	1609.3147	1609.3123	0.0024
(S−Se)-AVP	$C_{46}H_{65}N_{15}O_{12}SSe$	1131.3822	1131.3804	0.0018
Hg-bridged (S−Se)-AVP[a]	$C_{46}H_{65}HgN_{15}O_{12}SSe$	1331.3525	1331.3526	−0.0001
Bis-metalated (S−Se)-AVP[b]	$C_{48}H_{71}Hg_2N_{15}O_{12}SSe$	1563.3700	1563.3493	0.0207
Monometalated (S−Se)-AVP[b]	$C_{47}H_{69}HgN_{15}O_{12}SSe$	1347.3839	1347.3635	0.0204

[a]Formed with $HgCl_2$, CH_3HgCl, and Hg_2Cl_2. [b]Formed only with CH_3HgCl.

Under these conditions, the AVP peptide remained almost unreacted while high amounts of (Se−Se)- and (S−Se)-AVP were largely converted into the Hg-bridged adducts (Figure S32 and 7C). The formation of Hg-bridged peptide structures, after peptide incubation with calomel, indicated the change of Hg-oxidation state from +1 to +2, as postulated by Heyrovsky for an excess of Cys addition after the formation of the Hg_2Cys_2 complex.[25] The presence of DTT in the reaction medium can also promote the disproportionation of Hg(I) to Hg(0) and Hg(II),[46,47] followed by the subsequent complexation of Hg(II) to Se peptides.

Comparative Reactivity of AVP Peptides with Different Mercury Compounds. Figure 7 compares the reactivity of AVP peptides incubated for 18 h with 3 equiv of different mercury compounds. For each peptide, the proportion between the unreacted form and the sum of metalated forms is shown.

https://doi.org/10.1021/acs.inorgchem.3c01708
Inorg. Chem. 2023, 62, 14980−14990

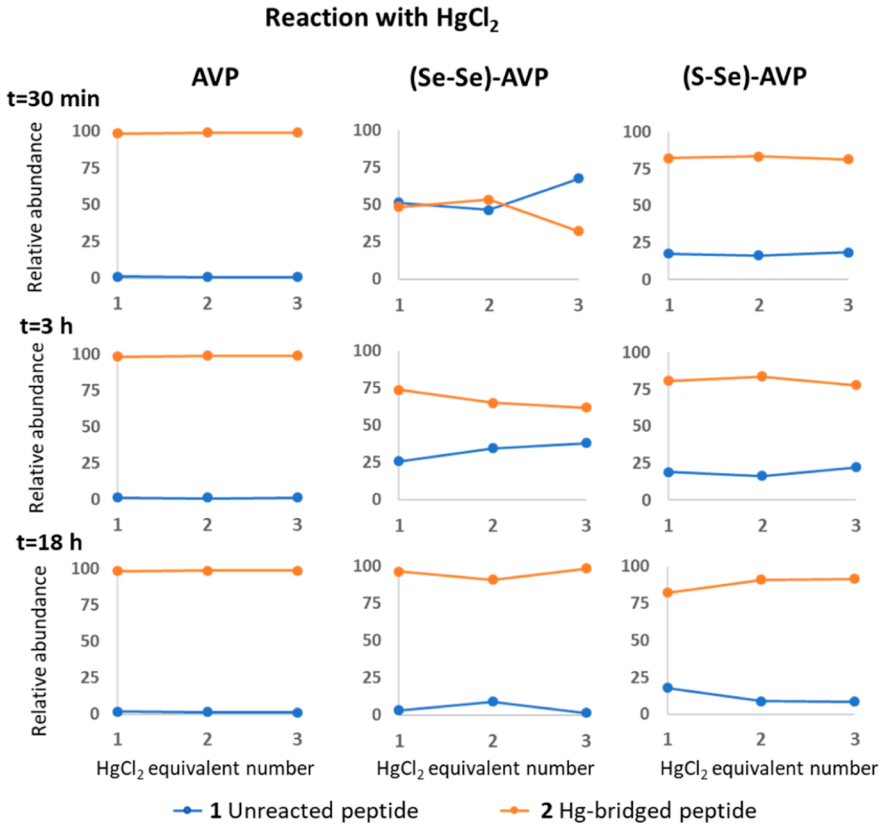

Figure 6. AVP peptides incubated at 37 °C in the presence of DTT with $HgCl_2$ (1−3 equiv) at 30 min, 3 and 18 h: % of unreacted and Hg-bridged peptides are reported as a function of $HgCl_2$ excess at different reaction times.

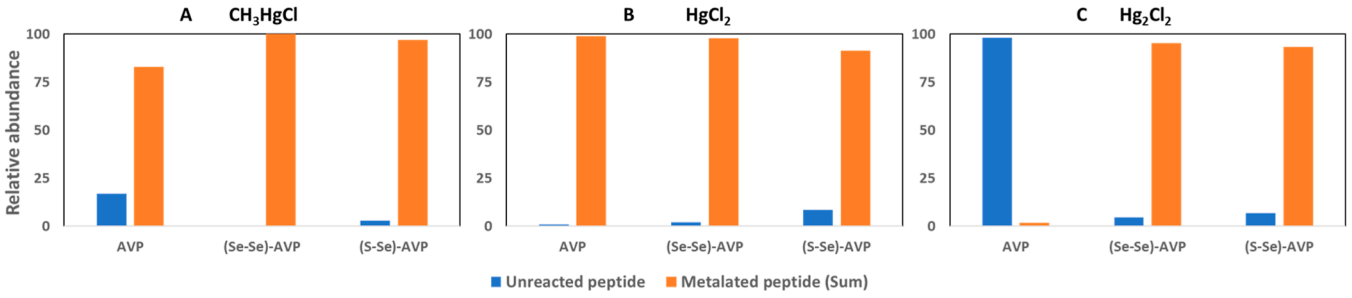

Figure 7. Relative abundance of unreacted and metalated (sum of adducts) AVP peptides incubated for 18 h at 37 °C in the presence of DTT with 3 equiv of (**A**) CH_3HgCl, (**B**) $HgCl_2$, or (**C**) Hg_2Cl_2.

It was concluded that the replacement of S by Se in vasopressin significantly increased its reactivity toward CH_3HgCl, while $HgCl_2$ did not favor its reaction with the Se peptide over the S peptide.

In the case of Hg_2Cl_2, which almost did not react with AVP while converting high amounts of (Se−Se)- and (S−Se)-AVP into the corresponding Hg-bridged species, the presence of at least one SeCys in the sequence of AVP seems to be essential for the metalation to occur.

Proposed Reaction Mechanism. The comparison of the reactivity of AVP peptides toward $HgCl_2$ and CH_3HgCl showed that, while $HgCl_2$ produced only bridged adducts, CH_3HgCl also resulted in mono- and/or bis-metalation. The propensity of $HgCl_2$ to form exclusively bridged adducts is probably related to the good leaving group ability of the second chloride ligand, while the C−Hg bond in CH_3HgCl cannot be readily hydrolyzed. Indeed, CH_3HgCl induced also the mono- or bis-metalation, **4** and **3**, respectively (Figure 8). Note that, in the case of (Se−Se)-AVP, the formation of the Hg-bridged adduct **2** was favored by an increase in the reaction time and an excess of CH_3HgCl.

After prolonged incubation time with CH_3HgCl, AVP formed almost exclusively the monometalated adduct **4**, while (S−Se)-AVP, as well as (Se−Se)-AVP, was converted into both the bis-metalated **3** and Hg-bridged **2** (prevalent) peptides. This underlies the high propensity of Se to promote a second reaction of the peptide with CH_3HgCl, by either an intramolecular- or intermolecular reactions, like in the case of the Hg-bridged **2** and bis-metalated **3** adduct formation, respectively.

Notably, this comparative analysis of the reactivity of the vasopressin analogues with CH_3HgCl suggests that the replacement of S by Se promotes the conversion of vasopressin into the Hg-bridged adduct by demethylation of CH_3HgCl.[48]

Competitive Reactivity Study. In order to assess the competition between S and Se forms of the peptide with CH_3HgCl, equimolar quantity of AVP (1 equiv), (Se−Se)-AVP

https://doi.org/10.1021/acs.inorgchem.3c01708
Inorg. Chem. 2023, 62, 14980−14990

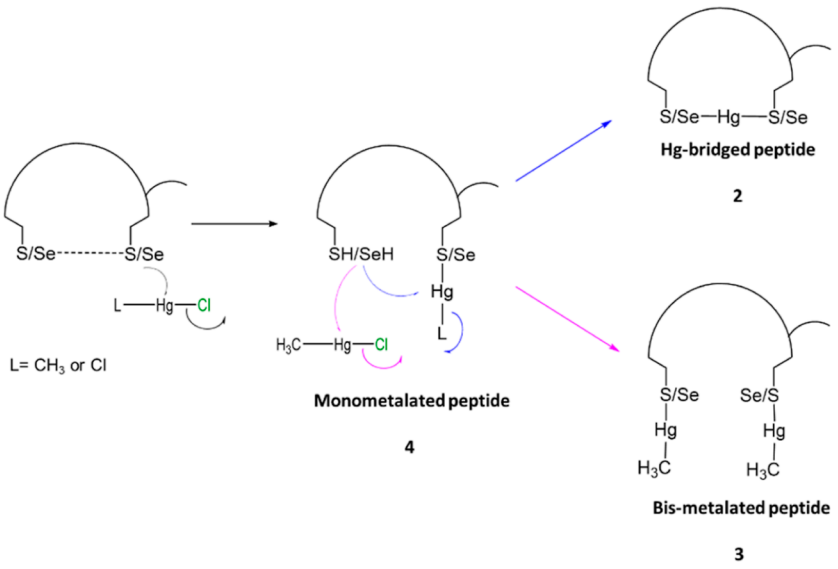

Figure 8. Proposed mechanism for the formation of Hg adducts with AVP peptides after the reaction with CH_3HgCl and $HgCl_2$ compounds.

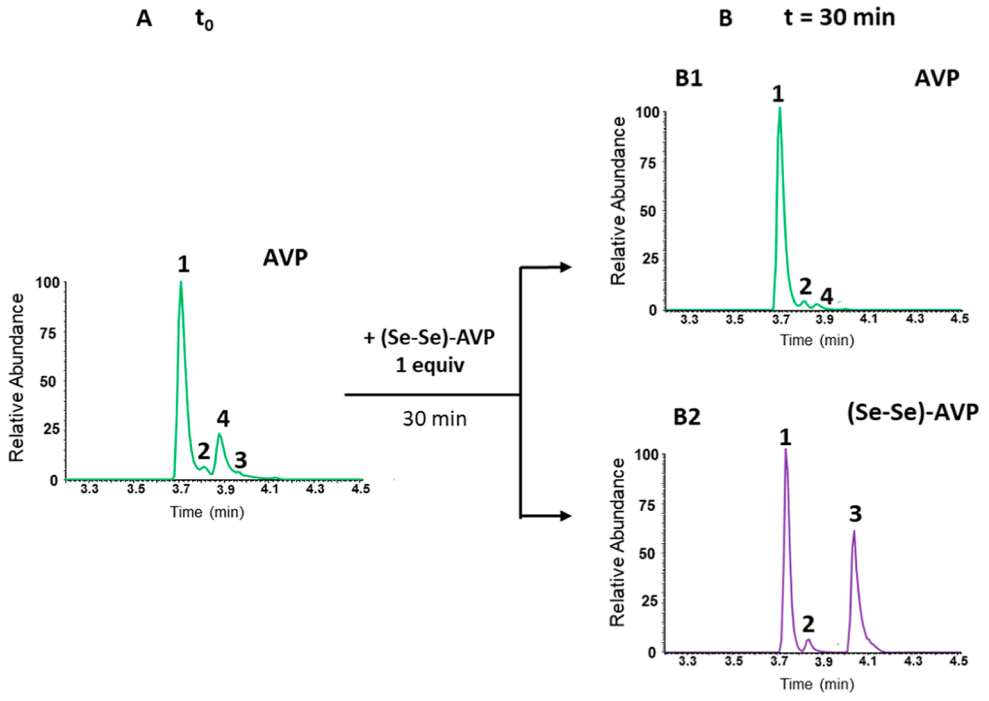

Figure 9. (**A**) LC−MS of AVP pre-treated with DTT and incubated with 1 equiv of CH_3HgCl at 37 °C during 18 h. XIC of ions m/z 542.72 (**1** AVP, t_R = 3.69 min), 643.71 (**2** Hg-bridged AVP, t_R = 3.78 min), 651,72 (**4** monometalated AVP adduct, t_R = 3.87 min), and 758.72 (**3** bis-metalated AVP adduct, t_R = 3.95 min). (**B**) LC−MS of pre-metalated AVP after incubation with 1 equiv of (Se−Se)-AVP at 37 °C during 30 min. **B(1)** XIC of AVP ions m/z 542.72 (**1** AVP, t_R = 3.69 min), 643.71 (**2** Hg-bridged AVP, t_R = 3.78 min), and 651.72 (**4** monometalated AVP adduct, t_R = 3,87 min). **B(2)** XIC of (Se−Se)-AVP ions m/z 590.67 (**1** (Se−Se)-AVP, t_R = 3.71 min), 690.65 (**2** Hg-bridged (Se−Se)-AVP, t_R = 3.81 min), and 805.66 (**3** bis-metalated (Se−Se)-AVP, t_R = 4.05).

(1 equiv) (both pre-treated with DTT), and CH_3HgCl (1 equiv) were simultaneously reacted at 37 °C for a time between 30 min and 18 h.

In the presence of its diselenide homologue, AVP was only slightly metalated, while the (Se−Se)-AVP was converted into Hg-bridged **2** and bis-metalated **3** adducts, whose ratio increased over incubation time (Figure S33).

The same experiment was repeated in the presence of higher quantities of AVP: 10-fold and 50-fold molar excess with respect to (Se−Se)-AVP (1 equiv) and CH_3HgCl (1 equiv). In the presence of 10-fold molar excess of AVP, diselenide vasopressin showed a high extent of metalation (Figure S34). Surprisingly, even in the presence of a 50-fold molar excess of AVP, the (Se−Se)-AVP still competed with its disulfide homologue in the binding with CH_3HgCl (Figure S35).

In conclusion, at the equimolar ratio, (Se−Se)-AVP was found to be more reactive toward CH_3Hg^+ than AVP and in the presence of a much larger amount of the latter, it was still able to be metalated by CH_3HgCl. This observation prompted us to investigate the ability of (Se−Se)-AVP to displace the CH_3Hg

https://doi.org/10.1021/acs.inorgchem.3c01708
Inorg. Chem. 2023, 62, 14980−14990

moiety from AVP. For this purpose, AVP (pre-reduced with DTT) was first incubated for 18 h with 1 equiv of CH_3HgCl in order to obtain its metalated adducts (Figure 9**A**) and then treated for 30 min with 1 equiv of (Se−Se)-AVP (pre-treated with DTT) (Figures S36 and 9B). After 30 min of reaction, AVP almost totally lost the CH_3Hg moiety bound to S (Figure 9**B**(**1**)), while (Se−Se)-AVP formed the bis metalated and the Hg-bridged adducts (Figure 9**B**(**2**)).

CONCLUSIONS

In this first experimental study of the comparative reactivity of Cys- and SeCys-containing biomolecules with different Hg compounds, we show that the replacement of S by Se in vasopressin drastically increased its reactivity toward CH_3HgCl. The reaction of (Se−Se)-AVP favored the formation of the Hg-bridged peptide by demethylation of CH_3HgCl. In competitive experiments, (Se−Se)-AVP readily and preferentially reacted with CH_3HgCl, showing a significant metalation extent even in the presence of a larger excess of its Cys homologue. On the basis of this result, we can hypothesize that this selenopeptide can affect the CH_3Hg^+ - protein thiol bonds believed to be responsible for the Hg toxicity. Moreover, (Se−Se)-AVP was able to displace almost totally the CH_3Hg moiety linked to S in AVP, which opens a perspective of using diselenide peptides as CH_3Hg^+ chelation agents. As an analogue of the natural hormone AVP, (Se−Se)-AVP can represent a potential lead compound for the development of methylmercury detoxification strategies.

ASSOCIATED CONTENT

Supporting Information

The Supporting Information is available free of charge at https://pubs.acs.org/doi/10.1021/acs.inorgchem.3c01708.

List of observed MS products and their structure, comparison of theoretical and experimental isotopic patterns, characterization of synthetic products (NMR and MS). LC−MS of AVP peptide reactivity with mercury compounds, and MS/MS of Hg-peptide adducts (PDF)

AUTHOR INFORMATION

Corresponding Author

Luisa Ronga − *Pays de l'Adour, E2S UPPA, CNRS, IPREM, 64000 Pau, France;* orcid.org/0000-0002-8485-6492; Email: luisa.ronga@univ-pau.fr

Authors

Mikel Bernabeu de Maria − *Pays de l'Adour, E2S UPPA, CNRS, IPREM, 64000 Pau, France*

Diego Tesauro − *Department of Pharmacy and CIRPeB, Università Degli Studi di Napoli Federico II, 49 80131 Naples, Italy*

Filippo Prencipe − *Istituto di Cristallografia (IC), CNR, 70126 Caserta, Italy*

Michele Saviano − *Istituto di Cristallografia (IC), CNR, 70126 Caserta, Italy;* orcid.org/0000-0001-5086-2459

Luigi Messori − *Department of Chemistry, Università Degli Studi di Firenze, 50019 Sesto Fiorentino, Italy;* orcid.org/0000-0002-9490-8014

Christine Enjalbal − *IBMM, Université de Montpellier, CNRS, ENSCM, UMR 5247, 34293 Montpellier Cedex 5, France;* orcid.org/0000-0003-4646-4583

Ryszard Lobinski − *Pays de l'Adour, E2S UPPA, CNRS, IPREM, 64000 Pau, France; Warsaw University of Technology, 00-664 Warsaw, Poland;* orcid.org/0000-0002-5644-4933

Complete contact information is available at: https://pubs.acs.org/10.1021/acs.inorgchem.3c01708

Author Contributions

The manuscript was written through contributions of all authors. All authors have given approval to the final version of the manuscript.

Notes

The authors declare no competing financial interest.

ACKNOWLEDGMENTS

M.B.d.M. acknowledges E2S-UPPA for the PhD fellowship. Financial support of the CNR for "The Bioinorganic Drugs (BIDs) joint laboratory: A multidisciplinary platform promoting new molecular targets for drug discovery" is acknowledged. Authors thank Dr. Simon Godin and Dr. Javier Jimenez Lamana for training M.B.d.M. in ESI− and ICP−MS, respectively.

REFERENCES

(1) Lamborg, C. H.; Hammerschmidt, C. R.; Bowman, K. L.; Swarr, G. J.; Munson, K. M.; Ohnemus, D. C.; Lam, P. J.; Heimbürger, L.-E.; Rijkenberg, M. J. A.; Saito, M. A. A Global Ocean Inventory of Anthropogenic Mercury Based on Water Column Measurements. *Nature* **2014**, *512*, 65−68.

(2) Selin, N. E. Global Biogeochemical Cycling of Mercury: A Review. *Annu. Rev. Environ. Resour.* **2009**, *34*, 43−63.

(3) Petrova, M. V.; Ourgaud, M.; Boavida, J. R. H.; Dufour, A.; Tesán Onrubia, J. A.; Lozingot, A.; Heimbürger-Boavida, L.-E. Human Mercury Exposure Levels and Fish Consumption at the French Riviera. *Chemosphere* **2020**, *258*, 127232.

(4) Xu, X.; Han, J.; Pang, J.; Wang, X.; Lin, Y.; Wang, Y.; Qiu, G. Methylmercury and Inorganic Mercury in Chinese Commercial Rice: Implications for Overestimated Human Exposure and Health Risk. *Environ. Pollut.* **2020**, *258*, 113706.

(5) Pearson, R. G. Hard and Soft Acids and Bases. *J. Am. Chem. Soc.* **1963**, *85*, 3533−3539.

(6) Ajsuvakova, O. P.; Tinkov, A. A.; Aschner, M.; Rocha, J. B. T.; Michalke, B.; Skalnaya, M. G.; Skalny, A. V.; Butnariu, M.; Dadar, M.; Sarac, I.; Aaseth, J.; Bjørklund, G. Sulfhydryl Groups as Targets of Mercury Toxicity. *Coord. Chem. Rev.* **2020**, *417*, 213343.

(7) Quig, D. Cysteine Metabolism and Metal Toxicity. *Alternative Med. Rev.* **1998**, *3*, 262−270.

(8) Starý, J.; Kratzer, K. Radiometric Determination of Stability Constants of Mercury Species Complexes with L-Cysteine. *Journal of Radioanalytical and Nuclear Chemistry Letters* **1988**, *126*, 69−75.

(9) Wang, F.; Lemes, M.; Khan, M. A. K. Metallomics of Mercury: Role of Thiol- and Selenol-Containing Biomolecules. In *Environmental Chemistry and Toxicology of Mercury*; Liu, G., Cai, Y., O'Driscoll, N., Eds.; John Wiley & Sons, Inc.: Hoboken, NJ, USA, 2011, pp 517−544. DOI: 10.1002/9781118146644.ch16.

(10) Sénèque, O.; Rousselot-Pailley, P.; Pujol, A.; Boturyn, D.; Crouzy, S.; Proux, O.; Manceau, A.; Lebrun, C.; Delangle, P. Mercury Trithiolate Binding (HgS_3) to a de Novo Designed Cyclic Decapeptide with Three Preoriented Cysteine Side Chains. *Inorg. Chem.* **2018**, *57*, 2705−2713.

(11) Mesterházy, E.; Lebrun, C.; Crouzy, S.; Jancsó, A.; Delangle, P. Short Oligopeptides with Three Cysteine Residues as Models of Sulphur-Rich Cu(i)- and Hg(ii)-Binding Sites in Proteins. *Metallomics* **2018**, *10*, 1232−1244.

(12) Ngu-Schwemlein, M.; Lin, X.; Rudd, B.; Bronson, M. Synthesis and ESI Mass Spectrometric Analysis of the Association of Mercury(II) with Multi-Cysteinyl Peptides. *J. Inorg. Biochem.* **2014**, *133*, 8−23.

(13) Steele, R. A.; Opella, S. J. Structures of the Reduced and Mercury-Bound Forms of MerP, the Periplasmic Protein from the Bacterial Mercury Detoxification System. *Biochemistry* **1997**, *36*, 6885−6895.
(14) Rossy, E.; Sénèque, O.; Lascoux, D.; Lemaire, D.; Crouzy, S.; Delangle, P.; Covès, J. Is the Cytoplasmic Loop of MerT, the Mercuric Ion Transport Protein, Involved in Mercury Transfer to the Mercuric Reductase? *FEBS Lett.* **2004**, *575*, 86−90.
(15) Ledwidge, R.; Patel, B.; Dong, A.; Fiedler, D.; Falkowski, M.; Zelikova, J.; Summers, A. O.; Pai, E. F.; Miller, S. M. NmerA, the Metal Binding Domain of Mercuric Ion Reductase, Removes Hg^{2+} from Proteins, Delivers It to the Catalytic Core, and Protects Cells under Glutathione-Depleted Conditions. *Biochemistry* **2005**, *44*, 11402−11416.
(16) Faller, P.; Ctortecka, B.; Tröger, W.; Butz, T.; Vašák, M. Optical and TDPAC Spectroscopy of Hg(II)-Rubredoxin: Model for a Mononuclear Tetrahedral [Hg(CysS)4]2− Center. *J. Biol. Inorg. Chem.* **2000**, *5*, 393−401.
(17) Chang, C.-C.; Lin, L.-Y.; Zou, X.-W.; Huang, C.-C.; Chan, N.-L. Structural Basis of the Mercury(II)-Mediated Conformational Switching of the Dual-Function Transcriptional Regulator MerR. *Nucleic Acids Res.* **2015**, *43*, 7612−7623.
(18) Song, S.; Li, Y.; Liu, Q. S.; Wang, H.; Li, P.; Shi, J.; Hu, L.; Zhang, H.; Liu, Y.; Li, K.; Zhao, X.; Cai, Z. Interaction of Mercury Ion (Hg2+) with Blood and Cytotoxicity Attenuation by Serum Albumin Binding. *J. Hazard. Mater.* **2021**, *412*, 125158.
(19) Simmons-Willis, T. A.; Koh, A. S.; Clarkson, T. W.; Ballatori, N. Transport of a Neurotoxicant by Molecular Mimicry: The Methylmercury−l-Cysteine Complex Is a Substrate for Human L-Type Large Neutral Amino Acid Transporter (LAT) 1 and LAT2. *Biochem. J.* **2002**, *367*, 239−246.
(20) Aschner, M.; Aschner, J. L.; Kimelberg, H. K. Methylmercury Neurotoxicity and Its Uptake Across the Blood — Brain Barrier. In *The Vulnerable Brain and Environmental Risks: Volume 2 Toxins in Food*; Isaacson, R. L., Jensen, K. F., Eds.; Springer US: Boston, MA, 1992, pp 3−17. DOI: 10.1007/978-1-4615-3330-6_1.
(21) Kajiwara, Y.; Yasutake, A.; Adachi, T.; Hirayama, K. Methylmercury Transport across the Placenta via Neutral Amino Acid Carrier. *Arch. Toxicol.* **1996**, *70*, 310−314.
(22) Pochini, L.; Peta, V.; Indiveri, C. Inhibition of the OCTN2 Carnitine Transporter by $HgCl_2$ and Methylmercury in the Proteoliposome Experimental Model: Insights in the Mechanism of Toxicity. *Toxicol. Mech. Methods* **2013**, *23*, 68−76.
(23) Galluccio, M.; Pochini, L.; Peta, V.; Iannì, M.; Scalise, M.; Indiveri, C. Functional and Molecular Effects of Mercury Compounds on the Human OCTN1 Cation Transporter: C50 and C136 Are the Targets for Potent Inhibition. *Toxicol. Sci.* **2015**, *144*, 105−113.
(24) Kanda, H.; Toyama, T.; Shinohara-Kanda, A.; Iwamatsu, A.; Shinkai, Y.; Kaji, T.; Kikushima, M.; Kumagai, Y. S-Mercuration of Rat Sorbitol Dehydrogenase by Methylmercury Causes Its Aggregation and the Release of the Zinc Ion from the Active Site. *Arch. Toxicol.* **2012**, *86*, 1693−1702.
(25) Heyrovský, M.; Mader, P.; Vavřička, S.; Veselá, V.; Fedurco, M. The Anodic Reactions at Mercury Electrodes Due to Cysteine. *J. Electroanal. Chem.* **1997**, *430*, 103−117.
(26) Gajdosechova, Z.; Mester, Z.; Feldmann, J.; Krupp, E. M. The Role of Selenium in Mercury Toxicity − Current Analytical Techniques and Future Trends in Analysis of Selenium and Mercury Interactions in Biological Matrices. *TrAC, Trends Anal. Chem.* **2018**, *104*, 95−109.
(27) Ralston, N. V. C.; Raymond, L. J. Mercury's Neurotoxicity Is Characterized by Its Disruption of Selenium Biochemistry. *Biochim. Biophys. Acta Gen. Subj.* **2018**, *1862*, 2405−2416.
(28) Carty, A.; Malone, S. F.; Taylor, N. J.; Canty', A. J. Synthesis, Spectroscopic, and X-Say Structural Characterization of Methylmercury-D, L-Selenocysteinate Monohydrate, a Key Model for the Methylmercury(II)-Selenoprotein Interaction. *J. Inorg. Biochem.* **1983**, *18*, 291−300.
(29) Taylor, N. J.; Wong, Y. S.; Chieh, P. C.; Carty, A. J.; Syntheses, X.-R. Syntheses, X-ray crystal structure, and vibrational spectra of L-cysteinato(methyl)mercury(II) monohydrate. *J. Chem. Soc., Dalton Trans.* **1975**, *5*, 438.
(30) Khan, M. A. K.; Asaduzzaman, A. Md.; Schreckenbach, G.; Wang, F. Synthesis, Characterization and Structures of Methylmercury Complexes with Selenoamino Acids. *Dalton Trans.* **2009**, *29*, 5766.
(31) Asaduzzaman, A. Md.; Khan, M. A. K.; Schreckenbach, G.; Wang, F. Computational Studies of Structural, Electronic, Spectroscopic, and Thermodynamic Properties of Methylmercury-Amino Acid Complexes and Their Se Analogues. *Inorg. Chem.* **2010**, *49*, 870−878.
(32) Valea, A.; Georgescu, C. E. Selenoproteins in Human Body: Focus on Thyroid Pathophysiology. *Hormones* **2018**, *17*, 183−196.
(33) Bernabeu de Maria, M.; Lamarche, J.; Ronga, L.; Messori, L.; Szpunar, J.; Lobinski, R. Selenol (-SeH) as a Target for Mercury and Gold in Biological Systems: Contributions of Mass Spectrometry and Atomic Spectroscopy. *Coord. Chem. Rev.* **2023**, *474*, 214836.
(34) Manceau, A.; Azemard, S.; Hédouin, L.; Vassileva, E.; Lecchini, D.; Fauvelot, C.; Swarzenski, P. W.; Glatzel, P.; Bustamante, P.; Metian, M. Chemical Forms of Mercury in Blue Marlin Billfish: Implications for Human Exposure. *Environ. Sci. Technol. Lett.* **2021**, *8*, 405−411.
(35) Pickering, I. J.; Cheng, Q.; Rengifo, E. M.; Nehzati, S.; Dolgova, N. V.; Kroll, T.; Sokaras, D.; George, G. N.; Arnér, E. S. J. Direct Observation of Methylmercury and Auranofin Binding to Selenocysteine in Thioredoxin Reductase. *Inorg. Chem.* **2020**, *59*, 2711−2718.
(36) Sugiura, Y.; Tamai, Y.; Tanaka, H. Selenium Protection against Mercury Toxicity: High Binding Affinity of Methylmercury by Selenium-Containing Ligands in Comparison with Sulfur-Containing Ligands. *Bioinorg. Chem.* **1978**, *9*, 167−180.
(37) Cordeau, E.; Arnaudguilhem, C.; Bouyssiere, B.; Hagège, A.; Martinez, J.; Subra, G.; Cantel, S.; Enjalbal, C. Investigation of Elemental Mass Spectrometry in Pharmacology for Peptide Quantitation at Femtomolar Levels. *PLoS One* **2016**, *11*, No. e0157943.
(38) Mobli, M.; Morgenstern, D.; King, G. F.; Alewood, P. F.; Muttenthaler, M. Site-Specific PKa Determination of Selenocysteine Residues in Selenovasopressin by Using 77Se NMR Spectroscopy. *Angew. Chem., Int. Ed.* **2011**, *50*, 11952−11955.
(39) Wenzel, M.; Casini, A. Mass Spectrometry as a Powerful Tool to Study Therapeutic Metallodrugs Speciation Mechanisms: Current Frontiers and Perspectives. *Coord. Chem. Rev.* **2017**, *352*, 432−460.
(40) Łobiński, R.; Schaumlöffel, D.; Szpunar, J. Mass Spectrometry in Bioinorganic Analytical Chemistry. *Mass Spectrom. Rev.* **2006**, *25*, 255−289.
(41) Koide, T.; Itoh, H.; Otaka, A.; Yasui, H.; Kuroda, M.; Esaki, N.; Soda, K.; Fujii, N. Synthetic Study on Selenocystine-Containing Peptides. *Chem. Pharm. Bull.* **1993**, *41*, 502−506.
(42) Kaiser, E.; Colescott, R. L.; Bossinger, C. D.; Cook, P. I. Color Test for Detection of Free Terminal Amino Groups in the Solid-Phase Synthesis of Peptides. *Anal. Biochem.* **1970**, *34*, 595−598.
(43) Hondal, R. J.; Nilsson, B. L.; Raines, R. T. Selenocysteine in Native Chemical Ligation and Expressed Protein Ligation. *J. Am. Chem. Soc.* **2001**, *123*, 5140−5141.
(44) Lamarche, J.; Alcoceba Álvarez, E.; Cordeau, E.; Enjalbal, C.; Massai, L.; Messori, L.; Lobinski, R.; Ronga, L. Comparative Reactivity of Medicinal Gold(i) Compounds with the Cyclic Peptide Vasopressin and Its Diselenide Analogue. *Dalton Trans.* **2021**, *50*, 17487−17490.
(45) Nikolaychuk, P. A. Is Calomel Truly a Poison and What Happens When It Enters the Human Stomach? A Study from the Thermodynamic Viewpoint. *Main Group Met. Chem.* **2016**, *39*, 41.
(46) Loux, N. T. An Assessment of Mercury-Species-Dependent Binding with Natural Organic Carbon. *Chem. Speciat. Bioavailab.* **1998**, *10*, 127−136.
(47) Vitello, J. D.; Pistone, D.; Cormier, A. D. A Problem Associated with the Use of a Calomel Reference Electrode in an ISE Analytical System. *Scand. J. Clin. Lab. Investig.* **1996**, *56*, 165−171.
(48) Khan, M. A. K.; Wang, F. Chemical Demethylation of Methylmercury by Selenoamino Acids. *Chem. Res. Toxicol.* **2010**, *23*, 1202−1206.

https://doi.org/10.1021/acs.inorgchem.3c01708
Inorg. Chem. 2023, 62, 14980−14990